Evolution of the Sun's large-scale magnetic field since the Maunder minimum

S. K. Solanki*, M. Schüssler* & M. Fligge†

* *Max-Planck-Institut für Aeronomie, D-37191 Katlenburg-Lindau, Germany*
† *Institut für Astronomie, ETH-Zentrum, CH-8092 Zürich, Switzerland*

The most striking feature of the Sun's magnetic field is its cyclic behaviour. The number of sunspots, which are dark regions of strong magnetic field on the Sun's surface, varies with a period of about 11 years. Superposed on this cycle are secular changes that occur on timescales of centuries and events like the Maunder minimum in the second half of the seventeenth century, when there were very few sunspots[1,2]. A part of the Sun's magnetic field reaches out from the surface into interplanetary space, and it was recently discovered[3] that the average strength of this interplanetary field has doubled in the past 100 years. There has hitherto been no clear explanation for this doubling. Here we present a model describing the long-term evolution of the Sun's large-scale magnetic field, which reproduces the doubling of the interplanetary field. The model indicates that there is a direct connection between the length of the sunspot cycle and the secular variations.

The magnetic field observed at the solar surface, a small part of which continues beyond the solar corona and permeates interplanetary space, is produced by a dynamo process operating in the solar interior. The field emerges at the surface in the form of bipolar regions embracing wide ranges of size and magnetic flux[4]; the larger of these are the active regions and the smallest are called ephemeral regions. These and other concepts are illustrated in Fig. 1.

Individual elements of the magnetic field (magnetic flux tubes or bundles of field lines) are transported by flows at the solar surface and carry out a combination of systematic motion and random walk (diffusion), so that part of the magnetic flux of the active region is spread widely over the solar surface right up to the poles[5,6]. The resulting large-scale pattern determines the global magnetic dipole moment and the strength of the field in interplanetary space[7,8]. Although the total amount of flux appearing on the solar surface in ephemeral regions is much bigger[9], the large-scale pattern of the field is mainly due to the large bipolar regions[5,10]. In fact, the net contribution of the ephemeral regions to the axial dipole moment of the Sun is a factor of 6 smaller than that of the large active regions[11]. Hence, for the simple approach taken here, it is sufficient to consider only the large active regions and follow the evolution of their magnetic flux. We are also restricted to the sunspot-bearing regions because the record of sunspot numbers is the only data set related to the solar magnetic field that reaches back to 1700. We note, however, that the influence of smaller bipolar regions is taken into account in a rough way; see equation (3) below.

In our model we consider the large-scale magnetic field (as measured, say, by the National Solar Observatory/Kitt Peak magnetograms[12]) to consist of two components: (1) (large) active regions and their early decay products (enhanced network, compare to Fig. 1); and (2) the part of the flux in the magnetic network that is organized into unipolar regions on a large enough scale for it to open into interplanetary space. As we are interested in the source of the interplanetary field we need not consider the closed part of the network flux.

Active region flux emerges rapidly (within days) and most of it is removed from the surface by cancellation at the border between opposite polarities within a few months[13]. We assume that a small part of the flux is transferred to the large-scale unipolar regions connected to the interplanetary field (which we call the open network) and resides there for a long time, of the order of years, in accordance with the observed long-term evolution of the large-scale field[5,6,8].

Owing to its short decay time, the (unsigned) magnetic flux in active regions, Φ_a, for our purpose can be assumed to be in quasi-steady balance between the relevant gain and loss terms: $E = T + \Phi_a/\tau_a$, where E is the flux emergence rate, $T = \Phi_a/\tau_t$ is

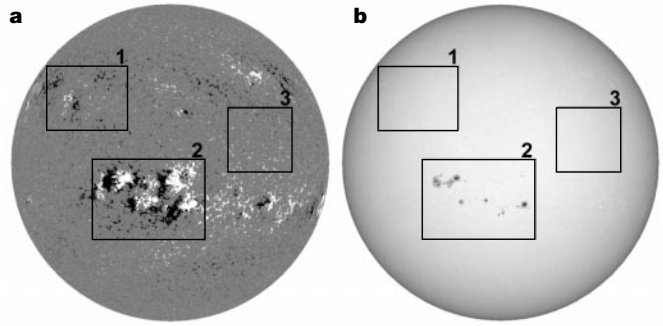

Figure 1 Distribution of the magnetic field and brightness on the solar surface. **a**, Magnetogram showing longitudinal magnetic field; **b**, filtergram showing brightness. Bright and dark features in the magnetograms represent magnetic flux of opposite polarity (that is, magnetic field directed out of and into the Sun, respectively); grey indicates the absence of net magnetic flux. The inserted frames 1–3 enclose features of particular interest. Frame 3 indicates a region of magnetic network (a 'salt and pepper' pattern in **a**, no dark sunspots in **b**). In frame 2, new magnetic flux has emerged from the solar interior to the surface and forms bipolar magnetic regions. These are identified by the large patches of field with opposite polarity and the sunspots visible in **b**. Only large bipolar regions form sunspots; they are called active regions. Their emergence rate varies strongly over the 11-year activity cycle of the Sun. Active regions begin to decay soon after the emergence of magnetic flux ceases. The sunspots break up and disappear within days or weeks, whereas the remainder of the active region often lives much longer in the form of the enhanced magnetic network (frame 1). Hence, the relative sunspot number, R, for which records exist back to 1700, can be used as a proxy for the flux emergence rate in studies of the long-term evolution of the large-scale solar magnetic field. Small bipolar regions without sunspots are referred to as ephemeral regions (data obtained by the Michelson-Doppler-Interferometer instrument[24] on board the Solar and Heliospheric Observatory, SOHO).

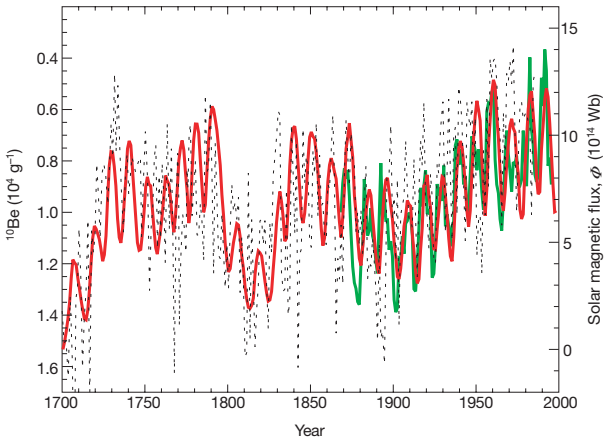

Figure 2 Evolution of the open magnetic flux at the solar surface since the end of the Maunder minimum in 1700. Data as predicted by our model are given by the red curve. For comparison, the flux of the interplanetary magnetic field[3] reconstructed from the geomagnetic variations (green curve) and the ^{10}Be concentration in ice cores[2] (dotted curve corresponding to the inverted scale on the left y-axis) are also plotted. The interplanetary flux values have been multiplied by a factor of 2 in order to obtain the total unsigned flux. The ^{10}Be record has been plotted without any smoothing or filtering.

the rate at which flux is transferred from active regions to the open network, with τ_t being the corresponding timescale, and τ_a is the decay time due to cancellation of opposite-polarity magnetic flux in the active region. The resulting expression for T can be inserted as a source term into the equation for the (unsigned) open network flux, Φ_o, yielding

$$\frac{d\Phi_o}{dt} = \gamma E - \frac{\Phi_o}{\tau_o} \quad (1)$$

with $\gamma = \tau_a/(\tau_a + \tau_t)$; τ_o is the decay timescale of the open network flux. We fix the value of γ using the flux emergence rate for the maximum of solar cycle 21 given by ref. 13. Requiring equality of Φ_o and the total unsigned interplanetary flux of approximately 1.4×10^{15} Wb during the maximum[3], we estimate γ by equating the two terms on the right-hand side of equation (1) for that value of Φ_o. This leaves τ_o as a free parameter of the model; the best fit to the reconstruction of ref. 3 is obtained with $\tau_o = 4$ yr (see below), which yields $\gamma \simeq 0.015$.

The flux emergence rate in active regions, E, is expressed in terms of the relative sunspot number, R, as

$$E = c\left(1 + \frac{A_f}{A_s}\right)R \quad (2)$$

where c is a conversion factor which can be determined from empirical emergence rates. The factor $(1 + A_f/A_s)$ takes into account that only a part of the newly emerged flux is in the form of sunspots (covering the area A_s), whereas the major part is concentrated in small magnetic elements, ensembles of which are visible as bright faculae and cover the area A_f. The observed linear relationship between magnetic flux and the corresponding area covered by bright features outside sunspots[13] supports our use of area as a proxy for magnetic flux. The ratio A_f/A_s in active regions varies over the solar cycle, being smaller at activity maximum than at minimum. Observations[14] and reconstructions of short-term solar irradiance variations[15] imply that:

$$\frac{A_f}{A_s}(R) = 21 + \frac{24.35}{R} - 0.061R \quad (3)$$

We note that A_f/A_s includes in a rough manner the contribution of small bipolar regions to flux emergence; through its nonlinear dependence on R it also takes into account to a certain extent that the number of small, relative to large, bipolar regions changes over the solar cycle. After substituting equations (2) and (3) into equation (1) the latter can be numerically integrated over any interval of time over which $R(t)$ is known.

If τ_o is sufficiently large, a secular variation of the open network flux is a natural consequence of our model. The cycle-averaged level of Φ_o depends not only on the total magnetic flux emerging during a cycle, Φ_{tot}, but also on the cycle length: shorter cycles lead to larger average open network flux (for constant Φ_{tot}). This can be simply illustrated by replacing the emergence term in equation (1) by a periodic function $a\Omega[1 + \cos(\Omega t)]$, where Ω is the cycle frequency. The amplitude factor, a, is multiplied by Ω in order to keep the total flux emerging per cycle independent of Ω. The resulting simplified version of equation (1) can be solved analytically. The open magnetic flux averaged over a cycle period asymptotically reaches the value:

$$\langle\Phi_o\rangle = a\Omega\tau_o \quad (4)$$

Hence, in addition to the cycle amplitude, the time-averaged open flux depends equally on the cycle length, with shorter cycles (larger Ω) yielding larger values of $\langle\Phi_o\rangle$. This effect is amplified by the anticorrelation between the length and the amplitude of the solar cycle[16,17].

In Fig. 2 we show Φ_o as reconstructed from the numerical solution of equation (1) since 1700, with $\tau_o = 4$ years (red curve). The year 1700 corresponds roughly to the end of the Maunder minimum. At that time very few sunspots were present on the solar surface[1], so there was little flux emerging in active regions and sufficient time for the large-scale unipolar flux previously present on the solar surface to decay. We have therefore set Φ_o to zero at 1700. We compare our result with the reconstruction of the interplanetary magnetic field of ref. 3 (green curve). The value of the decay time was adjusted to $\tau_o = 4$ yr in order to make the model match the relative amplitudes of the cyclic to the secular change exhibited by the interplanetary magnetic field. The agreement between the two quantities is gratifying, given the simplicity of our model and the assumptions entering the reconstruction.

The dotted curve in Fig. 2 represents the ^{10}Be concentration deduced from an ice core drilled at Dye 3, Greenland[2]. ^{10}Be is formed as a spallation product in the upper atmosphere of the Earth when cosmic rays hit nitrogen and oxygen nuclei. The ^{10}Be concentration is thus another measure of the solar magnetic activity, because a stronger, more complex solar magnetic field more efficiently shields the Earth from cosmic rays. Again, the agreement with our model is pleasing, and somewhat surprising in view of the unknown influence of past climate change on the ^{10}Be concentration. Not only are the secular behaviour of Φ_o and the ^{10}Be concentration almost identical, but also the ratio of cyclic to secular variations of Φ_o and the ^{10}Be data are compatible. This comparison also supports our choice of $\Phi_o = 0$ at 1700.

The resulting decay time of $\tau_o = 4$ yr allows for a significant redistribution of the open network flux by convection, differential rotation and meridional circulation during its lifetime[7,8]. This is in accordance with the accumulation of magnetic flux at high heliolatitudes during solar minimum as inferred from Ulysses measurements[18], which indicates that the residence time of magnetic flux must be sufficiently large for the meridional flow to concentrate the field at the poles. The polar fields dominate the interplanetary magnetic flux during solar activity minimum.

Our model yields a physical basis for understanding the secular trend of the interplanetary magnetic field detected in ref. 3. The decisive property of the model permitting the successful reproduction of the data is the long residence time of open magnetic flux at the solar surface. Considering only the instantaneous level of activity (say, the sunspot number) provides a very poor fit to the interplanetary field and the ^{10}Be data. Whereas the ^{10}Be data are dominated by a secularly changing background, the sunspot number always drops almost to zero at each activity minimum. An overlap between consecutive 'extended solar cycles'[19,20] could, in principle, introduce a secular trend by raising the minima between successive strong cycles; however, the small bipolar regions (ephemeral regions) that are mainly responsible for this overlap contribute very little to the large-scale patterns of the solar magnetic field[5,10] and the global dipole moment[11]. At most, this effect could lead to some decrease of the value of τ_o.

The correspondence between our model and the ^{10}Be record provides compelling evidence that the latter indeed tracks the interplanetary field[2] and thus gives a sound basis for taking the ^{10}Be record as a proxy of solar activity in the past. The model also introduces a mechanism for linking the solar cycle length[21] with secular variation of the interplanetary flux. Our reconstruction of the open solar magnetic flux provides the major parameter needed to reconstruct the secular variation of the cosmic ray flux impinging on the terrestrial atmosphere. It has been suggested that cosmic rays affect the total cloud cover of the Earth and thus drive the terrestrial climate[22,23]. The work presented here will allow further examination of this proposed link. □

Received 15 August; accepted 3 October 2000.

1. Ribes, J. C. & Nesme-Ribes, E. The solar sunspot cycle in the Maunder minimum AD1645 to AD1715. *Astron. Astrophys.* **276,** 549–563 (1993).
2. Beer, J., Blinov, A., Bonani, G., Hofmann, H. J. & Finkel, R. C. Use of ^{10}Be in polar ice to trace the 11-year cycle of solar activity. *Nature* **347,** 164–166 (1990).

3. Lockwood, M., Stamper, R. & Wild, M. N. A doubling of the Sun's coronal magnetic field during the past 100 years. *Nature* **399,** 437–439 (1999).
4. Harvey, K. L. & Zwaan, C. Properties and emergence of bipolar active regions. *Sol. Phys.* **148,** 85–118 (1993).
5. Sheeley, N. R. in *The Solar Cycle* (ed. Harvey, K. L.) 1–13 (Astronomical Society of the Pacific, ASP Conf. Series Vol. 27, San Francisco, 1992).
6. Wang, Y. M. & Sheeley, N. R. The rotation of photospheric magnetic fields: A random walk transport model. *Astrophys. J.* **430,** 399–412 (1994).
7. Wang, Y.-M., Lean, J. & Sheeley, N. R. The long-term variation of the Sun's open magnetic flux. *Geophys. Res. Lett.* **27,** 505–508 (2000).
8. Wang, Y.-M., Sheeley, N. R. & Lean, J. Understanding the evolution of the Sun's open magnetic flux. *Geophys. Res. Lett.* **27,** 621–624 (2000).
9. Schrijver, C. J. *et al.* Large-scale coronal heating by the small-scale magnetic field of the Sun. *Nature* **394,** 152–154 (1998).
10. Howard, R. & Labonte, B. J. Surface magnetic fields during the solar activity cycle. *Sol. Phys.* **74,** 131–145 (1981).
11. Harvey, K. L. in *Solar Surface Magnetism* (eds Rutten, R. J. & Schrijver, C. J.) 347–363 (Kluwer, Dordrecht, 1994).
12. Livingston, W. C., Harvey, J., Slaughter, C. & Trumbo, D. Solar magnetograph employing integrated diode arrays. *Appl. Opt.* **15,** 40–52 (1976).
13. Schrijver, C. J. & Harvey, K. L. The photospheric magnetic flux budget. *Sol. Phys.* **150,** 1–18 (1994).
14. Chapman, G. A., Cookson, A. M. & Dobias, J. J. Solar variability and the relation of facular to sunspot areas during solar cycle 22. *Astrophys. J.* **482,** 541–545 (1997).
15. Fligge, M., Solanki, S. K., Unruh, Y. C., Fröhlich, C. & Wehrli, C. A model of solar total and spectral irradiance variations. *Astron. Astrophys.* **355,** 709–718 (1998).
16. Dicke, R. H. Solar luminosity and the sunspot cycle. *Nature* **280,** 24–27 (1979).
17. Hoyng, P. Is the solar cycle timed by a clock? *Sol. Phys.* **169,** 253–264 (1996).
18. Wang, Y. M. & Sheeley, N. R. Solar implications of ULYSSES interplanetary field measurements. *Astrophys. J.* **447,** L143–L146 (1995).
19. Wilson, P. R., Altrock, R. C., Harvey, K. L., Martin, S. F. & Snodgrass, H. B. The extended solar activity cycle. *Nature* **333,** 748–750 (1988).
20. Harvey, K. L. in *The Solar Cycle* (ed. Harvey, K. L.) 335–367 (Astronomical Society of the Pacific, ASP Conf. Series Vol. 27, San Francisco, 1992).
21. Friis-Christensen, E. & Lassen, K. Length of the solar cycle: An indicator of solar activity closely associated with climate. *Science* **254,** 698–700 (1991).
22. Svensmark, H. & Friis-Christensen, E. Variation of cosmic ray flux and global cloud coverage—a missing link in solar-climate relationships. *J. Atmos. Terr. Phys.* **59,** 1225–1232 (1997).
23. Svensmark, H. Influence of cosmic rays on Earth's climate. *Phys. Rev. Lett.* **81,** 5027–5030 (1998).
24. Scherrer, P. H. *et al.* The Solar Oscillations Investigation—Michelson Doppler Imager. *Sol. Phys.* **162,** 129–188 (1995).

Acknowledgements

J. Beer and M. Lockwood provided the ^{10}Be record and the record of the reconstructed interplanetary magnetic field, respectively. We are grateful to K. Schrijver for comments on this paper.

Correspondence and requests for materials should be addressed to S.K.S. (e-mail: solanki@linmpi.mpg.de).

Coexistence of ferromagnetism and metallic conductivity in a molecule-based layered compound

Eugenio Coronado*, José R. Galán-Mascarós*†, Carlos J. Gómez-García* & Vladimir Laukhin*†

* *Instituto de Ciencia Molecular, Universidad de Valencia, Dr. Moliner 50, 46100 Burjasot, Spain*

Crystal engineering—the planning and construction of crystalline supramolecular architectures from modular building blocks—permits the rational design of functional molecular materials that exhibit technologically useful behaviour such as conductivity and superconductivity[1], ferromagnetism[2] and nonlinear optical properties[3]. Because the presence of two cooperative properties in the same crystal lattice might result in new physical phenomena and novel applications, a particularly attractive goal is the design of molecular materials with two properties that are difficult or impossible to combine in a conventional inorganic solid with a continuous lattice. A promising strategy for creating this type of 'bi-functionality' targets hybrid organic/inorganic crystals comprising two functional sub-lattices exhibiting distinct properties. In this way, the organic π-electron donor bis(ethylenedithio)tetrathiafulvalene (BEDT-TTF) and its derivatives, which form the basis of most known molecular conductors and superconductors[1], have been combined with molecular magnetic anions, yielding predominantly materials with conventional semiconducting or conducting properties[4,5], but also systems that are both superconducting and paramagnetic[6,7]. But interesting bulk magnetic properties fail to develop, owing to the discrete nature of the inorganic anions. Another strategy for achieving cooperative magnetism involves insertion of functional bulky cations into a polymeric magnetic anion, such as the bimetallic oxalato complex $[Mn^{II}Cr^{III}(C_2O_4)_3]^-$, but only insoluble powders have been obtained in most cases[8–12]. Here we report the synthesis of single crystals formed by infinite sheets of this magnetic coordination polymer interleaved with layers of conducting BEDT-TTF cations, and show that this molecule-based compound displays ferromagnetism and metallic conductivity.

The bimetallic complexes $[M^{II}M^{III}(C_2O_4)_3]^-$ (where M^{II} is Mn, Fe, Ni, Co, Cu; M^{III} is Cr, Fe, Ru; and $(C_2O_4)^{2-}$ is the oxalate dianion) form infinite layers of oxalate-bridged hexagonal networks in the presence of bulky organic cations of the type $[XR_4]^+$ (where X is N, P; and R is Ph, *n*-Pr, *n*-Bu), which act as templates for the formation of the net (Fig. 1a)[10]. The magnetic properties of these coordination polymers are of interest, as they behave as ferro-, ferri- or canted antiferromagnets with critical temperatures ranging from 5 to 44 K (refs 11, 12). Moreover, it is possible to replace the electronically 'inactive' organic cations by paramagnetic organometallic cations[8], metal complexes exhibiting spin crossover, or organic dyes that give rise to nonlinear optical properties[9].

We prepared crystals of composition $[BEDT\text{-}TTF]_3[MnCr(C_2O_4)_3]$ by electrocrystallization of a methanol/benzonitrile/dichloromethane solution containing the tris-oxalate Cr(III) complex (0.01 M) and the Mn(II) ion in a ratio 2:3 and a suspension of BEDT-TTF, which was slowly oxidized at a constant current of

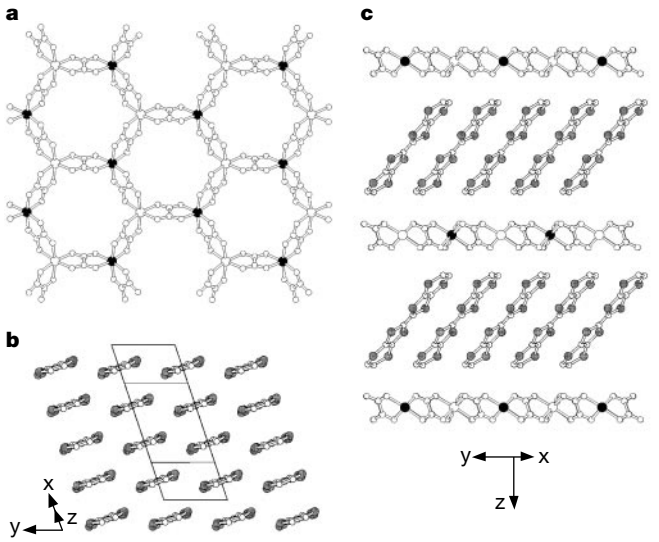

Figure 1 Structures of the hybrid material and the two sublattices. **a**, View of the $[M^{II}M^{III}(C_2O_4)_3]^-$ bimetallic layers. Filled and open circles in the vertices of the hexagons represent the two types of metals. **b**, Structure of the organic layer, showing the β packing of the BEDT-TTF molecules. **c**, Representation of the hybrid structure along the *c* axis, showing the alternating organic/inorganic layers.

† Present addresses: Department of Chemistry, Texas A&M University, College Station, Texas, USA (J.R.G.-M.); ICMB-CSIC, Campus de la UAB, 08193 Bellaterra, Spain (V.L.).